REGULAR SAMPLING OF TENSOR SIGNALS: THEORY AND APPLICATION TO fMRI

Charilaos I. Kanatsoulis*, Nicholas D. Sidiropoulos*, Mehmet Akçakaya*, and Xiao Fu[†]

*Department of ECE, University of Minnesota, Minneapolis, MN, USA *Department of ECE, University of Virginia, Charlottesville, VA, USA †School of EECS, Oregon State University, Corvallis, OR, USA

ABSTRACT

Sampling lies at the heart of signal processing. The celebrated Shannon - Nyquist theorem states that in order to reconstruct a continuous or discrete time signal from uniform samples one must sample at a rate twice the highest frequency present in the signal. Numerous signals and images of interest, however, are not even approximately bandlimited. While much progress has happened in recent years, reconstruction from sub-Nyquist samples still hinges on the use of random / incoherent (aggregate) sampling patterns, instead of uniform or regular sampling, which is far more simple, practical, and natural in many applications. In this work, we study regular sampling and reconstruction of three- or higher-dimensional signals (tensors). We prove that exact tensor reconstruction from regular samples is feasible under mild conditions on the rank of the tensor. Furthermore we cast the functional magnetic resonance imaging (fMRI) acceleration task as a regular tensor sampling problem and provide an algorithmic framework that effectively handles the reconstruction task. Experiments based on synthetic data and real fMRI data showcase the effectiveness of our approach.

Index Terms— sampling, reconstruction, tensor completion, MRI acceleration, functional MRI

1. INTRODUCTION

In the first half of the 20th century, Whittaker, Nyquist, Kotelnikov, and Shannon [1, 2, 3, 4] laid the foundation of the sampling theorem, which together with the discovery of the fast Fourier transform catalyzed the field of signal processing. In order to perfectly reconstruct a signal from uniformly spaced samples, one must sample at a rate at least twice the maximum frequency present in the signal. The theorem applies to both continuous and discrete time bandlimited signals. The Shannon-Nyquist theorem is one of very few results that guarantee perfect reconstruction of a signal after a regular, and more specifically uniform, sampling process. Unfortunately, many time series, images, and higher-dimensional (e.g., video) signals of practical interest are nowhere close to being bandlimited.

Compressive sensing (CS) [5, 6, 7] emerged in the early 2000's as an alternative which allows recovery from a set of measurements sampled or compressed below the Nyquist rate. CS relies on two basic principles: the signal of interest must be sparse in some domain and the sampling/compression pattern should be 'incoherent'. Compared to the sampling theorem, CS exploits sparsity (instead of bandlimitedness) in a known domain, thereby enabling reconstruction from fewer measurements. The drawback is that one loses the simplicity of regular sampling, which is also the only practical way to sample in many applications. Following similar principles as in

Supported in part by U.S. NSF grants IIS-1447788, IIS-1704074, ECCS 1808159 and CCF-1651825, and NIH grant P41EB015894.

CS, low rank matrix completion (LRMC) studies sampling and reconstruction of two dimensional discrete signals (matrices, such as images). The basic property utilized is low matrix rank, and incoherent sampling patterns are again employed. CS and LRMC are linked to a number of important engineering applications, such as collaborative filtering. However, the incoherence requirement on the sampling process is restrictive indeed – it does not apply in various practical scenarios.

Naturally, CS and LRMC ideas have been extended to higher dimensional signals and in particular tensors. Sampling and reconstruction of multidimensional signals is an important problem. In magnetic resonance imaging (MRI) or functional MRI (fMRI), for instance, the agonizingly slow scan acquisition process strongly motivates exploring appropriate sampling techniques for acceleration. Several works have appeared on the topic of tensor completion and reconstruction, e.g., [8, 9, 10, 11, 12, 13]. The majority of them focuses on algorithmic aspects of tensor completion [8, 10, 11, 12], or attempt to generalize ideas such as the nuclear norm and singular value decomposition (SVD) to tensors [13]. The few that propose models and provable conditions under which tensor completion is feasible, adopt a LRMC type of analysis [9], which however is not tailored to the unique properties of tensors. Most importantly, the proposed tensor sampling techniques use random samples or random projections, and have difficulty dealing with regular sampling patterns.

Recent work by Sorensen et. al. [14, 15] considers the problem of completing a tensor with missing fibers, which is common in chemometrics, and provides theoretical conditions under which completion of a tensor with missing fibers is feasible – as well as an algebraic framework to handle the problem. The work in [14] is the first, to the best of our knowledge, that can handle systematic fiber sampling; but the algebraic approach therein is derived under a noiseless setting and real-world data are usually quite noisy. Moreover, a variety of other interesting types of regular tensor sampling have not been considered. For example, a different type of regular aggregate sampling was considered in [16, 17, 18].

Contributions: We study the task of sampling and reconstruction of third order tensors. Our approach focuses on using *possibly multiple* regular fiber and slab sampling patterns, in one or multiple modes of the tensor. Unlike CS and LRMC, that hinge on incoherent sampling strategies, we offer provable conditions for tensor reconstruction from regular and/or equispaced samples, under mild rank limitedness conditions. Our analysis leverages the uniqueness properties of the canonical polyadic decomposition (CPD) of tensors. Furthermore we cast the task of parallel fMRI acceleration as a regular tensor sampling and reconstruction procedure and propose an efficient algorithmic framework to tackle it. Numerical experiments using synthetic and real data show that the proposed approach is very promising.

2. TENSOR ALGEBRA PRELIMINARIES

We now briefly review basic concepts of tensor algebra that are necessary for exposition of our main contributions. We refer the interested reader to [19, 20] for more in-depth background.

Third order tensors $\underline{X} \in \mathbb{C}^{I \times J \times K}$, are three way arrays indexed by i, j, k. A third order tensor has 3 modes: columns $\underline{X}(i, :, k)$, rows $\underline{X}(:,j,k)$ and fibers $\underline{X}(i,j,:)$, and 3 types of slabs: vertical, horizontal and frontal slabs, represented by $\underline{X}(:,j,:)$, $\underline{X}(i,:,:)$, X(:,:,k) respectively. Any third order tensor can be decomposed as a sum of three way outer products, i.e., $\underline{X}(i,j,k) =$ $\sum_{f=1}^{F} A(i,f)B(j,f)C(k,f)$. This model is known as the canonical polyadic decomposition (CPD), where F is the tensor rank or CP rank and $A \in \mathbb{C}^{I \times F}$, $B \in \mathbb{C}^{J \times F}$, and $C \in \mathbb{C}^{K \times F}$ are called the low-rank factors of the third order tensor. For brevity we use the notation $\underline{X} = \llbracket A, B, C
rbracket$ to represent the CPD of a tensor. A salient feature of tensors is that the CPD model is essentially unique even when F is much larger than $\max\{I, J, K\}$.

Theorem 1 [21] Let $\underline{X} = [\![A, B, C]\!]$ with $A : I \times F$, $B : J \times F$, and $C: K \times F$. Assume that A, B and C are drawn from some joint absolutely continuous distribution. Also assume $I \geq J \geq K$ without loss of generality. If $F \leq 2^{\lfloor \log_2 J \rfloor + \lfloor \log_2 K \rfloor - 2}$, then the decomposition of \underline{X} in terms of A, B, and C is essentially unique, almost surely.

Here, essential uniqueness means that A, B, C are identifiable up to column permutation and scaling. The above uniqueness condition is mild. For instance, consider a $200 \times 200 \times 200$ tensor. Following Theorem 1, it admits an essentially unique CPD if $F \leq 4096$. This uniqueness condition is way more relaxed compared to those for matrix factorization, which require nonnegativity, sparsity, geometric conditions, and rank lower than the outer dimensions [22, 23, 24].

One useful operation in tensor algebra is mode multiplication. The mode product operation multiplies a matrix to a tensor in one mode. Specifically, $\underline{\tilde{X}} = \underline{X} \times_1 P_1 \times_2 P_2 \times_3 P_3$ multiplies each column, row and fiber of the tensor by P_1 , P_2 , P_3 respectively.

3. THE TENSOR SAMPLING MODEL

The core of this paper discusses the reconstruction of a third order tensor from regular samples taken from one or different modes of the tensor. The claim is fundamental: regular samples are enough to recover a third order tensor as long as the tensor is sufficiently low rank. To make the claim more concrete, let us consider two different sampling paradigms.

3.1. Tensor sampling paradigm 1

In the first paradigm we study the case where equispaced slabs are taken from two different modes of a third order tensor. Instead of the

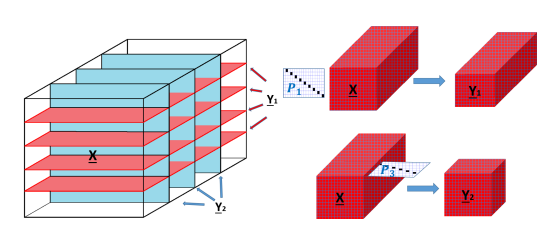


Fig. 1: Tensor sampling paradigm 1.

full tensor, we observe an equispaced subset of frontal and horizontal slabs. To be more precise, let $\underline{X} \in \mathbb{C}^{I \times J \times K}$ be the original full tensor, which is not fully accessible. Then $\underline{Y}_1 \in \mathbb{C}^{I_r \times J \times K}$ represents the subset of observable horizontal slabs of \underline{X} and $\underline{Y}_2 \in \mathbb{C}^{I \times J \times K_r}$ contains the subset of observable frontal slabs. \underline{Y}_1 can be written the subset of observable frontal slabs. ten as the mode 1 multiplication of tensor \underline{X} with selection matrix $P_1 \in \mathbb{R}^{I_r \times I}$, i.e.

$$\mathbf{P}_1 \in \mathbb{R}^{I_r \times I}$$
, i.e. $\underline{\mathbf{Y}}_1 = \underline{\mathbf{X}} \times_1 \mathbf{P}_1$ (1)

and \underline{Y}_2 as a mode 3 multiplication with matrix $P_3 \in \mathbb{R}^{K_r \times K}$, i.e.

$$\underline{\boldsymbol{Y}}_2 = \underline{\boldsymbol{X}} \times_3 \boldsymbol{P}_3 \tag{2}$$

A schematic illustration of tensor sampling paradigm 1 model is given in Fig. 1. Note that P_1 , P_3 are fat matrices, which perform slab selection in one mode of \underline{X} , thus $I_r < I$, $K_r < K$.

Now, since X is a third order tensor, it admits a CPD model of rank F, i.e. $\underline{X} = [\![A,B,C]\!]$. Following (1), (2), \underline{Y}_1 , \underline{Y}_2 can be represented in the form:

$$\underline{Y}_1 = \llbracket P_1 A, B, C \rrbracket, \ \underline{Y}_2 = \llbracket A, B, P_3 C \rrbracket$$
 (3)

Regarding the identifiability of tensor sampling paradigm 1, we have the following theorem:

Theorem 2 Let $X \in \mathbb{C}^{I \times J \times K}$ be the original tensor signal, with CPD $\underline{X} = [\![A, B, C]\!]$, and I_r , K_r be the number of horizontal and frontal slabs that we sample/observe. Assume that A, B and C are drawn from a joint absolutely continuous distribution, and that $(A^{\star}, B^{\star}, C^{\star})$ satisfies the equations in (3). Also assume that $I_r K \geq I K_r$ without loss of generality. Then, $\hat{\boldsymbol{X}}(i,j,k) =$ $\sum_{f=1}^{F} \mathbf{A}^{\star}(i,f) \mathbf{B}^{\star}(j,f) \mathbf{C}^{\star}(k,f)$ recovers the ground-truth $\underline{\mathbf{X}}$ almost surely if $F \leq \min\left\{2^{\lfloor \gamma_1 \rfloor - 2}, 2^{\lfloor \gamma_2 \rfloor - 2}, JK_r\right\}$, where $\gamma_1 = \log_2(I_r J)$, $\gamma_2 = \log_2(I_r K)$.

3.2. Tensor sampling paradigm 2

The second tensor sampling paradigm considers the scenario where equispaced samples are taken along a single mode of the tensor. The schematic illustration of tensor paradigm 2 is given in Fig. 2.

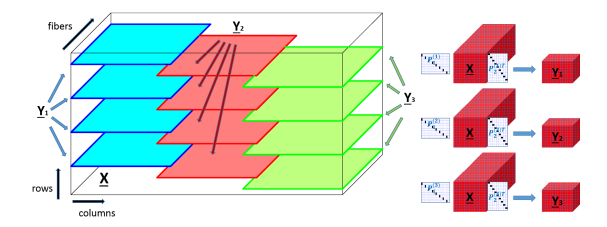


Fig. 2: Tensor sampling paradigm 2.

In particular, we sample the original tensor using r different patterns of horizontal sub-slab samples – in Fig. 2, r = 3. Each pattern observes I/r equispaced rows of the tensor over (J/r+1) columns - forming therefore a group of horizontal sub-slabs. Each pair of patterns includes common columns and samples are taken from all columns, rows and fibers of the tensor (in a regular manner). These are necessary conditions on the sampling. First, for pairwise mutually exclusive patterns, there exists a non-trivial scaling ambiguity, which cannot be determined, and second, completely unobserved slabs are impossible to recover. Note that tensor sampling paradigm 2 can be alternatively viewed as a special case of fiber sampling, where fibers appear in r overlapping and regularly-spaced sampling patterns. This will become more clear in the following subsection.

Following similar analysis as in paradigm 1 we deduce:

$$\underline{Y}_1 = \underline{X} \times_1 P_1^{(1)} \times_2 P_2^{(1)} = [P_1^{(1)} A, P_2^{(1)} B, C]$$
 (4a)

$$\underline{Y}_2 = \underline{X} \times_1 P_1^{(2)} \times_2 P_2^{(2)} = \left[P_1^{(2)} A, P_2^{(2)} B, C \right]$$
 (4b)

$$\underline{\boldsymbol{Y}}_{3} = \underline{\boldsymbol{X}} \times_{1} \boldsymbol{P}_{1}^{(3)} \times_{2} \boldsymbol{P}_{2}^{(3)} = \left[\boldsymbol{P}_{1}^{(3)} \boldsymbol{A}, \boldsymbol{P}_{2}^{(3)} \boldsymbol{B}, \boldsymbol{C} \right]$$
(4c)

Regarding the identifiability of tensor sampling paradigm 2, we have the following theorem:

Theorem 3 Let $\underline{X} \in \mathbb{C}^{I \times J \times K}$ be the original tensor signal, with CPD $\underline{X} = [\![A, B, C]\!]$, which we sample according to tensor sampling paradigm 2, using r patterns. Assume that A, B and C are drawn from a joint absolutely continuous distribution, and that (A^*, B^*, C^*) satisfies equations (4). Then, $\underline{\hat{X}}(i, j, k) = \sum_{f=1}^F A^*(i, f)B^*(j, f)C^*(k, f)$ recovers the ground-truth \underline{X} almost surely if $F \leq \min\left\{2^{\lfloor \gamma_1 \rfloor - 2}, 2^{\lfloor \gamma_2 \rfloor - 2}, 2^{\lfloor \gamma_3 \rfloor - 2}\right\}$, where $\gamma_1 = \log_2(\frac{IJ}{r^2})$, $\gamma_2 = \log_2(\frac{IK}{r})$, $\gamma_3 = \log_2(\frac{K_T}{r})$.

The proofs of the Theorems 2, 3 are relegated to a journal version due to space limitations. The implication is striking. If the original tensor \underline{X} is sufficiently low rank, then the sub-sampled tensors admit a unique CPD. The proof uses Theorem 1 to establish identifiability on the CPD of the sub-sampled tensors and the coupling between sub-tensor to reconcile for permutation/scaling mismatches. Then one can identify the latent factors A, B, C from the sub-sampled tensors and reconstruct the original tensor as $\underline{X} = [\![A,B,C]\!]$. To get an idea on the theoretical conditions, consider the following example. Let $\underline{X} \in \mathbb{C}^{200 \times 200 \times 200}$ be a tensor that we sample according to paradigm 2 with r=3, as illustrated in Fig. 4. Reconstruction is guaranteed, under the assumptions of Theorem 3, if the CP rank of X satisfies $F \leq 1024$.

3.3. Application to parallel fMRI

Interestingly tensor sampling paradigm 2 finds application in accelerating fMRI scan acquisition. An fMRI raw scan, is a tensor signal with usually 2 spatial dimensions in k-space (k_x , k_y) and time, coils as additional dimensions. Acquiring high spatial resolution fMRI is challenging due to time restrictions. In ongoing efforts to cut down on the scan acquisition time (and motion artifacts due to patient discomfort), research has focused on accelerating the scanning process by undersampling the k_y frequencies. Classic methods, mainly used for MRI scans, use learning and calibration type techniques [25, 26, 27], while others employ the CS framework [26, 28, 29] or LRMC [29, 30, 31] to perform the reconstruction.

While MRI offers complete freedom in choosing the frequencies to acquire at each time slot (as long as the number remains the same and the same sampling pattern is followed in every coil), fMRI is performed using a special fast imaging acquisition that is practically only used with equispaced sub-sampling patterns due to restrictions associated with magnetic field inhomogenities and Eddy currents. A realistic fMRI sampling example with 3-fold acceleration is given in Fig. 3. First a fully sampled scan is acquired and then 1/3 of

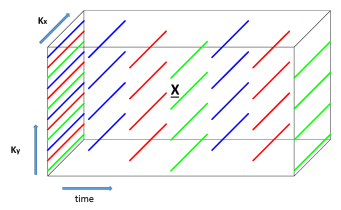


Fig. 3: fMRI sampling at a single coil.

 k_y frequencies is sampled at each time slot. This process reduces the operational time between consecutive time slots by a factor of 3. Note that an initial fully sampled scan is typical in fMRI (for calibration) and in our case it reconciles for scaling mismatches.

The accelerated fMRI acquisition is a regular tensor sampling process. This becomes clear by appropriately rearranging the time

domain in the sampling of Fig. 3 and forming it as the tensor sampling paradigm of Fig. 2. Note that such a sampling process might be tricky for classic techniques. On the one hand, calibration-based techniques such as GRAPPA [25] are linear and suffer from noise amplification at high acceleration rates. On the other hand, CS and LRMC schemes have difficulties in operating with regular samples, since their success rests upon incoherent sampling. Our proposed tensor approach offers a theoretical framework that allows reconstruction by sampling equispaced frequencies and in the next section we propose an algorithmic framework to tackle the reconstruction problem. We should mention here that tensor approaches have been proposed in the context of MRI denoising [32] or dynamic MRI sampling, e.g. [33]. However, regarding MRI sampling, they neither discuss reconstruction guarantees nor work with regular samples.

4. TENSOR COMPLETION FROM REGULAR SAMPLES USING COUPLED TENSOR FACTORIZATION

In this section we briefly discuss the algorithmic component of our approach. More detailed discussion is postponed for the journal version due to space limitations. In both sampling paradigms we propose to employ a coupled tensor factorization approach. In particular for paradigm 1 we propose the following estimator:

$$\underset{\boldsymbol{A},\boldsymbol{B},\boldsymbol{C}}{\text{minimize}} \ \|\underline{\boldsymbol{Y}}_{1} - [\![\boldsymbol{P}_{1}\boldsymbol{A},\boldsymbol{B},\boldsymbol{C}]\!]\|_{F}^{2} + \|\underline{\boldsymbol{Y}}_{2} - [\![\boldsymbol{A},\boldsymbol{B},\boldsymbol{P}_{3}\boldsymbol{C}]\!]\|_{F}^{2}, \ (5)$$

whereas for paradigm 2 we propose the following formulation:

$$\underset{\boldsymbol{A},\boldsymbol{B},\boldsymbol{C}}{\text{minimize}} \left\| \underline{\boldsymbol{Y}}_{1} - \left[\left[\boldsymbol{P}_{1}^{(1)} \boldsymbol{A}, \boldsymbol{P}_{2}^{(1)} \boldsymbol{B}, \boldsymbol{C} \right] \right] \right\|_{F}^{2} + \left\| \underline{\boldsymbol{Y}}_{2} - \left[\left[\boldsymbol{P}_{1}^{(2)} \boldsymbol{A}, \boldsymbol{P}_{2}^{(2)} \boldsymbol{B}, \boldsymbol{C} \right] \right] \right\|_{F}^{2} + \left\| \underline{\boldsymbol{Y}}_{3} - \left[\left[\boldsymbol{P}_{1}^{(3)} \boldsymbol{A}, \boldsymbol{P}_{2}^{(3)} \boldsymbol{B}, \boldsymbol{C} \right] \right] \right\|_{F}^{2} \right\}$$
(6)

There are several ways to handle the above non-convex problems. We employ tensorlab's structured data fusion (SDF) [34], which uses a nonlinear least squares (NLS) approach. We also cleverly initialize the coupled procedure with the factors produced by the CPD of each sampled tensor and taking into consideration the shared factors.

4.1. REgular Tensor Sampling and Interpolation Algorithm (RETSINA)

For the fMRI sampling and reconstruction task we use a slightly different approach tailored to the specific application. First we observe that the raw fMRI scan is originally a fourth order tensor. It would be straight forward to extend our previous analysis to fourth order tensors, however in this paper we prefer to unfold the 4-way fMRI tensor to a 3-way one by concatenating k_x and k_y space into one dimension. Assuming the first dimension to be the k-space, the second one to be the time domain and coils as the third dimension, the previously explained sampling strategy falls exactly under the framework of tensor sampling paradigm 2. The REgular Tensor Sampling and INterpolation Algorithm (RETSINA) is presented in Algorithm 1. We follow a 3 step procedure, which reduces the operational time of the algorithm, and empirically yields enhanced reconstruction accuracy. In step 1 (initialization), for r-fold acceleration we sum every r vertical sub-sampled slabs across the time dimension (assuming the missing values are represented with zeros) and obtain a tensor $\underline{\boldsymbol{X}}_r \in \mathbb{C}^{I \times J/r \times K}$ without missing entries. This way we are able to get a rough estimate of A, C factors. In step 2 (refinement), we compute the CPD of $\underline{\boldsymbol{Y}}_1$ (initialized by step 1) and the CPD of $\{\underline{Y}_i\}_{i\neq 1}$ with C constant. Finally, in step 3, we compute the final factors by solving (6) with tensorlab's SDF.

5. SIMULATIONS

In this section, we showcase the effectiveness of the proposed Tensor Sampling framework using synthetic as well as real data experiments. All simulations are performed in MATLAB on a Linux server with 3.6GHz cores and 32GB RAM.

Algorithm 1: RETSINA

Input: $r, F, \underline{\tilde{X}}$: incomplete tensor (zeros are missing entries). Initialization: $\underline{X}_r(:,j,:) = \sum_{l=(j-1)r+2}^{} \underline{\tilde{X}}(:,l,:)$ $A, C \leftarrow \text{CPD}(\underline{X}_r)$ Form $\{\underline{Y}_i\}_{i=1}^r \text{ from } \underline{\tilde{X}} \text{ and set } \mathcal{S}_i = [1,i+1:r:J].$ $B(\mathcal{S}_i,:) = P_2^{(i)}B = \arg\min_{Z} \|\underline{Y}_i - [\![P_1^{(i)}A,Z,C]\!]\|_F^2$ Refinement: $P_1^{(1)}A, P_2^{(1)}B, C \leftarrow \text{CPD}(\underline{Y}_1).$ $P_1^{(i)}A, P_2^{(i)}B, \sim \leftarrow \text{CPD}(\underline{Y}_i), \quad i \neq 1.$ Solve (6) using tensorlab's NLS algorithm. Reconstruct the missing entries of X using $\hat{X} = [\![A,B,C]\!]$.

5.1. Synthetic Experiments

In this subsection we conduct synthetically generated experiments to examine the performance of the proposed framework when tensor sampling paradigm 1 is performed. In particular, we generated a tensor $\underline{X} \in \mathbb{R}^{200 \times 300 \times 400}$ as $\underline{X} = [\![A, B, C]\!]$, where the elements of the factor matrices are drawn from an independent identically distributed (i.i.d.) zero mean, unit variance Gaussian distribution. For the experiments, we set $I_r = I/r$, $K_r = K/r$, where r is the downsampling factor, and vary the tensor rank F from 200 to 500 and r from 2 to 100. To evaluate the performance of tensor reconstruction, we measure the normalized root mean squared error, i.e.

$$\text{NRMSE} = \frac{\sum_{k=1}^K \lVert \hat{\underline{\boldsymbol{X}}}(:,:,k) - \underline{\boldsymbol{X}}(:,:,k) \rVert_F}{\sum_{k=1}^K \lVert \underline{\boldsymbol{X}}(:,:,k) \rVert_F}$$

The results are shown in Fig. (4). As expected the reconstruction

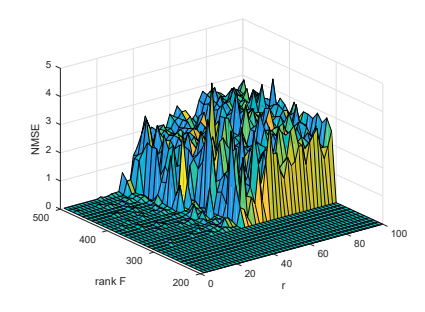


Fig. 4: rank F vs downsampling factor r.

is deteriorating as the rank F or the factor r are increasing. For reasonably small ranks and high downsampling ratio $(\frac{\# \text{samples}}{IJK})$ the reconstruction is almost perfect.

5.2. Accelerated parallel fMRI

In this subsection we test the performance of the proposed RETSINA with real fMRI scans, fully sampled in the k-space. The dataset is obtained from the Center for Magnetic Resonance Research (CMRR) at the University of Minnesota. The raw scan is a fourth order tensor of size $104 \times 104 \times 32 \times 490$ and we unfold it as a third order tensor $\underline{X} \in \mathbb{C}^{10816 \times 32 \times 490}$. The sampling pattern performs 3-fold acceleration as illustrated in Fig. 3. We choose F=100 and run step 1, 2, 3 for 50, 2 and 10 iterations respectively. The baseline algorithms used for comparison are k-t Focuss [29], which is a CS type algorithm, k-t SLR [31] which combines ideas from both LRMC and CS, and the zero padding inverse discrete Fourier transform (IDFT). Note that k-t SLR works in the real

x-y-time domain and thus we measure the NRMSE of the absolute valued IDFT of the scan, denoted as NRMSE₂, for fair comparisons. For both k-t Focuss and k-t SLR the publicly available code was used. Note that k-t Focuss and k-t SLR are single coil algorithms, thus we treated each coil separately. k-t SLR requires parameter tuning and so we used a validation step to tune effectively.

Table 1 measures the NRMSE in k-space and absolute real space as well as runtime. It is clear that the proposed RETSINA achieves the best accuracy in the k-space whereas it works comparably well (but markedly faster) with k-t SLR in the absolute real space. This is expected since RETSINA reconstructs the k-space and k-t SLR the magnitude of the IDFT. In terms of runtime IDFT is the fastest but fails to reconstruct the image. RETSINA on the other hand works faster than k-t SLR and k-t Focuss. However, parallel implementation could significantly speed up k-t Focuss and k-t SLR operation time at the cost of computational resources.

Table 1: Reconstruction performance of the competing algorithms.

Algorithm	RETSINA	k-t Focuss	k-t SLR	IDFT
NRMSE	0.124	0.339	1.41	0.8156
$NRMSE_2$	0.081	0.286	0.073	0.7376
runtime	12min	25.6min (48sec/coil)	480min (15min/coil)	14sec

Fig. 5 shows the reconstructed fMRI scans at different time frames produced by RETSINA along with the fully sampled data. The quality of the reconstruction is significantly high, rendering the proposed RETSINA a good alternative for fMRI acceleration. Fi-

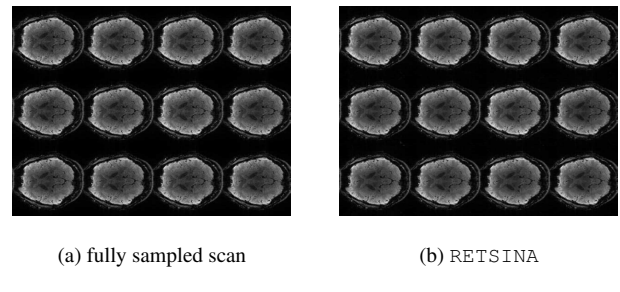


Fig. 5: fMRI reconstruction with 3-fold acceleration

nally, in Fig. 6 we illustrate the reconstruction performance at a single frame for the competing algorithms. Note that k-t SLR seems to work comparably well, although being slightly off in contrast.

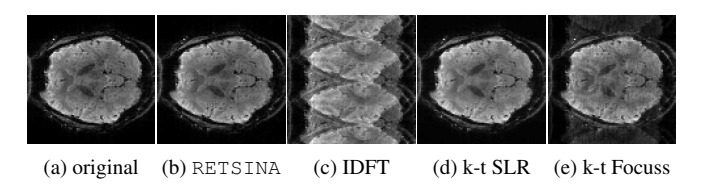


Fig. 6: Reconstruction at a single frame

6. CONCLUSION

In this work we studied regular sampling and reconstruction on three-dimensional signals. Compared to CS, LRMC, as well as other tensor works, we provide provable conditions under which reconstruction of the tensor can be achieved from regular or even equispaced samples. Furthermore, we cast the fMRI acceleration task as a regular tensor sampling process and provided an efficient algorithmic framework to approach the problem. Simulations with synthetic data as well as real fMRI scans in the k-space show the validity and effectiveness of our work.

7. REFERENCES

- [1] E. T. Whittaker, "On the functions which are represented by the expansions of the interpolation-theory," *Proceedings of the Royal Society of Edinburgh*, vol. 35, pp. 181–194, 1915.
- [2] H. Nyquist, "Certain topics in telegraph transmission theory," *Transactions of the American Institute of Electrical Engineers*, vol. 47, no. 2, pp. 617–644, 1928.
- [3] V. A. Kotelnikov, "On the transmission capacity of the 'ether' and of cables in electrical communications," in *Proceedings of the first All-Union* Conference on the technological reconstruction of the communications sector and the development of low-current engineering. Moscow. Citeseer, 1933.
- [4] C. E. Shannon, "Communication in the presence of noise," *Proceedings of the IRE*, vol. 37, no. 1, pp. 10–21, 1949.
- [5] E. J. Candès, J. Romberg, and T. Tao, "Robust uncertainty principles: Exact signal reconstruction from highly incomplete frequency information," *IEEE Transactions on information theory*, vol. 52, no. 2, pp. 489–509, 2006.
- [6] D. L. Donoho, "Compressed sensing," *IEEE Transactions on information theory*, vol. 52, no. 4, pp. 1289–1306, 2006.
- [7] E. J. Candès and M. B. Wakin, "An introduction to compressive sampling," *IEEE signal processing magazine*, vol. 25, no. 2, pp. 21–30, 2008
- [8] J. Liu, P. Musialski, P. Wonka, and J. Ye, "Tensor completion for estimating missing values in visual data," *IEEE transactions on pattern analysis and machine intelligence*, vol. 35, no. 1, pp. 208–220, 2013.
- [9] S. Gandy, B. Recht, and I. Yamada, "Tensor completion and low-n-rank tensor recovery via convex optimization," *Inverse Problems*, vol. 27, no. 2, p. 025010, 2011.
- [10] N. Vervliet, O. Debals, L. Sorber, and L. De Lathauwer, "Breaking the curse of dimensionality using decompositions of incomplete tensors: Tensor-based scientific computing in big data analysis," *IEEE Signal Processing Magazine*, vol. 31, no. 5, pp. 71–79, 2014.
- [11] G. Tomasi and R. Bro, "Parafac and missing values," *Chemometrics and Intelligent Laboratory Systems*, vol. 75, no. 2, pp. 163–180, 2005.
- [12] E. Acar, D. M. Dunlavy, T. G. Kolda, and M. Mørup, "Scalable tensor factorizations for incomplete data," *Chemometrics and Intelligent Laboratory Systems*, vol. 106, no. 1, pp. 41–56, 2011.
- [13] M. Yuan and C.-H. Zhang, "On tensor completion via nuclear norm minimization," *Foundations of Computational Mathematics*, vol. 16, no. 4, pp. 1031–1068, 2016.
- [14] M. Sørensen and L. De Lathauwer, "Fiber sampling approach to canonical polyadic decomposition and tensor completion," ESAT-STADIUS, KU Leuven, Belgium, Tech. Rep., pp. 15–151, 2017.
- [15] M. Sørensen, N. D. Sidiropoulos, and L. De Lathauwer, "Canonical polyadic decomposition of a tensor that has missing fibers: A monomial factorization approach," submitted to *ICASSP 2019*.
- [16] C. I. Kanatsoulis, X. Fu, N. D. Sidiropoulos, and W.-K. Ma, "Hyperspectral super-resolution: A coupled tensor factorization approach," arXiv preprint arXiv:1804.05307, 2018.
- [17] —, "Hyperspectral super-resolution via coupled tensor factorization: Identifiability and algorithms," in 2018 IEEE International Conference on Acoustics, Speech and Signal Processing (ICASSP). IEEE, 2018, pp. 3191–3195.
- [18] —, "Hyperspectral super-resolution: Combining low rank tensor and matrix structure," in 2018 25th IEEE International Conference on Image Processing (ICIP). IEEE, 2018, pp. 3318–3322.
- [19] N. D. Sidiropoulos, L. De Lathauwer, X. Fu, K. Huang, E. E. Papalexakis, and C. Faloutsos, "Tensor decomposition for signal processing and machine learning," *IEEE Transactions on Signal Processing*, vol. 65, no. 13, pp. 3551–3582, 2017.
- [20] T. G. Kolda and B. W. Bader, "Tensor decompositions and applications," SIAM review, vol. 51, no. 3, pp. 455–500, 2009.

- [21] L. Chiantini and G. Ottaviani, "On generic identifiability of 3-tensors of small rank," SIAM Journal on Matrix Analysis and Applications, vol. 33, no. 3, pp. 1018–1037, 2012.
- [22] X. Fu, K. Huang, B. Yang, W.-K. Ma, and N. D. Sidiropoulos, "Robust volume minimization-based matrix factorization for remote sensing and document clustering," *IEEE Transactions on Signal Processing*, vol. 64, no. 23, pp. 6254–6268, 2016.
- [23] X. Fu, K. Huang, and N. D. Sidiropoulos, "On identifiability of nonnegative matrix factorization," arXiv preprint arXiv:1709.00614, 2017.
- [24] X. Fu, K. Huang, N. D. Sidiropoulos, and W.-K. Ma, "Nonnegative matrix factorization for signal and data analytics: Identifiability, algorithms, and applications," *IEEE Signal Processing Magazine, feature* article, to appear, Oct.2018.
- [25] M. A. Griswold, P. M. Jakob, R. M. Heidemann, M. Nittka, V. Jellus, J. Wang, B. Kiefer, and A. Haase, "Generalized autocalibrating partially parallel acquisitions (grappa)," Magnetic Resonance in Medicine: An Official Journal of the International Society for Magnetic Resonance in Medicine, vol. 47, no. 6, pp. 1202–1210, 2002.
- [26] M. Lustig and J. M. Pauly, "Spirit: iterative self-consistent parallel imaging reconstruction from arbitrary k-space," *Magnetic resonance* in medicine, vol. 64, no. 2, pp. 457–471, 2010.
- [27] M. Akçakaya, S. Moeller, S. Weingärtner, and K. Uğurbil, "Scanspecific robust artificial-neural-networks for k-space interpolation (raki) reconstruction: Database-free deep learning for fast imaging," *Magnetic resonance in medicine*, 2018.
- [28] R. Otazo, D. Kim, L. Axel, and D. K. Sodickson, "Combination of compressed sensing and parallel imaging for highly accelerated firstpass cardiac perfusion mri," *Magnetic resonance in medicine*, vol. 64, no. 3, pp. 767–776, 2010.
- [29] H. Jung, K. Sung, K. S. Nayak, E. Y. Kim, and J. C. Ye, "k-t focuss: a general compressed sensing framework for high resolution dynamic mri," *Magnetic resonance in medicine*, vol. 61, no. 1, pp. 103–116, 2009.
- [30] P. J. Shin, P. E. Larson, M. A. Ohliger, M. Elad, J. M. Pauly, D. B. Vigneron, and M. Lustig, "Calibrationless parallel imaging reconstruction based on structured low-rank matrix completion," *Magnetic resonance in medicine*, vol. 72, no. 4, pp. 959–970, 2014.
- [31] S. G. Lingala, Y. Hu, E. DiBella, and M. Jacob, "Accelerated dynamic mri exploiting sparsity and low-rank structure: kt slr," *IEEE transactions on medical imaging*, vol. 30, no. 5, pp. 1042–1054, 2011.
- [32] B. Yaman, S. Weingärtner, N. Kargas, N. D. Sidiropoulos, and M. Akcakaya, "Locally low-rank tensor regularization for high-resolution quantitative dynamic mri," in *Computational Advances in Multi-Sensor Adaptive Processing (CAMSAP)*, 2017 IEEE 7th International Workshop on. IEEE, 2017, pp. 1–5.
- [33] M. Mardani, G. B. Giannakis, and K. Ugurbil, "Tracking tensor subspaces with informative random sampling for real-time mr imaging," arXiv preprint arXiv:1609.04104, 2016.
- [34] N. Vervliet, O. Debals, L. Sorber, M. Van Barel, and L. De Lathauwer, "Tensorlab v3. 0, march 2016," *URL: http://www. tensorlab. net*.